2018-03-02

Haloferax volcanii Proteome Response to Deletion of a Rhomboid Protease Gene

Costa, MI

http://hdl.handle.net/10026.1/11853

==

Haloferax volcanii proteome response to deletion of a rhomboid protease gene

Mariana I. Costa[1¥], Micaela Cerletti[1¥], Roberto A. Paggi[1], Christian Trötschel[2], Rosana E. De Castro[1], Ansgar Poetsch[2, 3 *] and María I. Giménez[1*].

[1]Instituto de Investigaciones Biológicas, Universidad Nacional de Mar del Plata (UNMdP). Consejo Nacional de Investigaciones Científicas y Técnicas (CONICET), Funes 3250 4to nivel, (7600) Mar del Plata, Provincia de Buenos Aires, Argentina. [2]Plant Biochemistry, Faculty of Biology & Biotechnology, Ruhr University Bochum, 44801 Bochum, Germany. [3] School of Biomedical and Healthcare Sciences, Plymouth University, Plymouth PL4 8AA, United Kingdom

Key words: *Archaea*, *Haloferax volcanii*, rhomboid protease, shotgun proteomics, protease substrate.

Abstract

Rhomboids are conserved intramembrane serine proteases involved in cell signaling processes. Their role in prokaryotes is scarcely known and remains to be investigated in *Archaea*. We previously constructed a rhomboid homolog deletion mutant (Δ*rhoII*) in *Haloferax volcanii,* which showed reduced motility, increased novobiocin sensitivity and an N- glycosylation defect. To address the impact of *rhoII* deletion on *H. volcanii* physiology, the proteomes of mutant and parental strains were compared by shotgun proteomics. A total of 1847 proteins were identified (45.8 % of *H. volcanii* predicted proteome) from which 103 differed in amount. Additionally, the

mutant strain evidenced 99 proteins with altered electrophoretic migration, suggesting differential

post-translational processing/modification. Integral membrane proteins that evidenced variations in

concentration, electrophoretic migration and/or semi-tryptic cleavage in the mutant were considered

as potential RhoII targets. These included a PrsW protease homolog (which was less stable in the

mutant strain), a predicted halocyanin and six integral membrane proteins potentially related to the

mutant glycosylation (S-layer glycoprotein, Agl15) and cell adhesion/motility (flagellin1,

HVO_1153, PilA1 and PibD) defects. This study investigated for the first time the impact of a

rhomboid protease on the whole proteome of an organism.

Introduction

Proteases cleave their protein/peptide substrates in an irreversible reaction and through this activity

they catalyze the fate and activity of other proteins. They control appropriate protein folding,

localization, activation (or inactivation) and shedding from cell surfaces. Therefore, proteases

control a wide range of important cellular functions including DNA replication, cell cycle

progression, cell proliferation, cell-cell communication, differentiation, morphogenesis, neuronal

outgrowth, homeostasis, wound healing, immunity, angiogenesis and apoptosis[1, 2].

Intramembrane proteolysis, that is, the cleavage of peptide bonds within the plane of the cell

membrane, is a mechanism conserved in the three Domains of Life. The genomes of every

sequenced organism encode for intramembrane proteases (IMPs). These enzymes exert diverse

biological functions and are considered as promising future drug targets[3]. Among IMPs, three major

classes have been described, the GxGD-aspartyl proteases (eukaryal signal peptide peptidase SPP

and presenilin families), rhomboids and site 2 proteases (S2P)[2].

Rhomboid proteases (Rho) are widespread serine proteases and to date they are the best understood

IMPs[4]. In eukaryotic organisms they have been implicated in a variety of processes. In *Drosophila melanogaster* a Rho activates epidermal growth factor receptors[5, 6]. In mitochondria the mammalian PARL rhomboid protease regulates cell homeostasis and has been implicated in the biology of diabetes and Parkinson´s disease[7]. Rhomboids in parasites regulate adhesion to the host through processing of adhesins[8]. Recently a role in fungal hypoxia adaptation through sterol regulatory element-binding protein activation has been reported[9].

In prokaryotes, the role of Rho has been explored to a lesser extent. Up to date, the function of only one prokaryotic Rho, AarA from *Providencia stuartii*, has been elucidated. AarA cleaves an N-terminal extension of the twin arginine translocation (Tat) complex component TatA, allowing for the assembly of a functional Tat translocon and, hence, for the export of a still unidentified *quorum sensing* signal[10]. In addition, some bacterial rhomboid deletion mutants have been characterized, even though no specific protease substrates were reported. A null mutant in the *Escherichia coli* rhomboid protease GlpG showed no evident phenotype under laboratory conditions, except for a mild increase in resistance to cefotaxime. However, GlpG was shown to cleave heterologous substrates. Specific targets of other Rho, such as Spitz, Gurken and Keren of *D. melanogaster,* were proteolytically processed by GlpG[11]. A chimeric protein, consisting of the N-terminal and periplasmically localized β-lactamase domain, a LacY-derived transmembrane segment (TMS) and a cytoplasmic maltose binding protein domain, could be cleaved *in vitro* by this Rho[12] and, in addition, GlpG could cleave truncated forms of the transporter protein MdfA[13]. In *Bacillus subtilis* a rhomboid protease gene (*yqgP*) null mutant displayed a cell division defect and decreased glucose uptake[14]. *Mycobacterium smegmatis* rhomboid null mutants exhibited impaired biofilm formation and augmented antibiotic sensitivity[15].

The Rho family is widely represented through archaeal genomes[16]. Particularly, the halophilic model archaeon *Haloferax volcanii* encodes two Rho homologs, HVO_1474 (RhoI) and HVO_0727 (RhoII). We have previously obtained and characterized a Rho mutant deleted in the *rhoII* gene in

H. volcanii. The mutant strain (MIG1) showed reduced motility on soft agar plates, increased novobiocin sensitivity and a truncation in a novel oligosaccharide bound to position N732 of the S-layer glycoprotein (SLG)[17]. However, global changes on the proteome that may explain these phenotypes still need to be determined.

Comparative proteomics is a valuable tool to analyze the impact of the absence/overexpression of a particular protease on the proteome of a certain organism and allows for identification of putative endogenous substrates. In the case of processive proteases, accumulation of a particular protein in a protease defective strain with respect to the control strain would be an evidence of that protein being a specific substrate. This method was applied by our group to identify candidate targets of the LonB protease in *H. volcanii*[18]. On the other hand, the situation for regulatory enzymes, such as Rho, is different. These proteases cut at specific sites releasing or exposing fragments of the substrate, and therefore, protease activity may be evidenced by changes in electrophoretic migration and/or stability of the (unprocessed) substrate protein.

In this work, a quantitative high-throughput comparative proteomics approach was applied in *H. volcanii* to understand the importance of Rho in archaeal physiology and to identify putative natural targets of RhoII.

Experimental Section

Strains and growth conditions

H. volcanii H26 (DS70 Δ*pyrE2*)[19] and MIG1[17] were grown in MGM 18% or Hv-Min medium[20] at 42 °C and 150 rpm. When needed, uracil or tryptophan (50 µg/ml) was added to Hv-Min.

E. coli DH10β (Invitrogen) and GM33 (Marinus, 1973) were grown in Luria-Bertani (LB) medium

at 37 °C and 150 rpm. Kanamycin (50 μg/ml) or ampicillin (100 μg/ml) was added to the medium when indicated. *E. coli* cells were transformed by the CaCl$_2$ method[21].

Cell fractionation

H. volcanii cultures were grown up to the indicated optical density at 600 nm (OD$_{600}$) and cells were harvested by centrifugation (10,000 x*g* 10 min, 4 °C). Culture medium was re-centrifuged under the same conditions and the supernatant was passed through a 0.22 μm nitrocellulose filter and precipitated with TCA 10% (v/v). Precipitated proteins were washed twice with 80% (v/v) acetone and left to dry 30 min at room temperature. Cell pellets were resuspended in 50 mM HCl-Tris, 2 M NaCl (pH 7.5) and disrupted by ultrasound (3 x 30 s, 80 W). Lysates were clarified (17,000 x*g* for 20 min at 4 °C) and membranes were pelleted by centrifugation (100,000 x*g* for 1 h at 4 °C). The membranes were washed with the same buffer and both, supernatant (cytoplasmic fraction) and membranes, were re-centrifuged for 30 min in the same conditions. To remove remaining salts, cytoplasm and membrane proteins were precipitated overnight with 100% acetone at 4 °C followed by centrifugation (17,000 x*g* for 20 min at 4 °C). The precipitated proteins were washed twice with 80% (v/v) and once with 100% acetone and left to dry for 30 min at room temperature. All samples were resuspended in 1x SDS-PAGE loading buffer[22] containing 0.1% (w/v) SDS and 0.1 M DTT, incubated for 10 min at 70 °C and conserved at -20 °C until used.

SDS-PAGE

Samples (30 μg per lane) were loaded onto 10% (w/v) polyacrylamide gels containing 0.1% SDS. The gels were run at room temperature (20 mA) until samples passed the stacking gel and all proteins were concentrated into one protein band in the separation gel. For the PROTOMAP assay[23], samples were allowed to run 2 cm beyond the stacking gel (Fig. S1). Proteins were visualized with a coomassie brilliant blue (CBB-G250) stain[24].

In-gel tryptic digestion

Protein bands were excised from the gels and cut into small cubes (ca. 1×1 mm) which were completely destained according to Schluesener and colleagues[25]. In the case of PROTOMAP assay, each lane was divided in four 0.5 cm sections which were treated separately in the same manner (Figure 1). Gel pieces were dried by incubation with 100% acetonitrile for 10 min at room temperature and then incubated with 50 mM DTT in 25 mM NH_4HCO_3 (30 min at 60 °C) to reduce proteins disulfide bonds. The gel pieces were dried again with acetonitrile and proteins were alkylated treating the gel pieces with 50 mM iodoacetamide in 25 mM NH_4HCO_3 (1 h at room temperature in darkness). After washing (with destaining solution) and drying the gel pieces in a SpeedVac, trypsin (porcine, sequencing grade, Promega) solution (12.5 ng ml^{-1} in 25 mM ammonium bicarbonate, pH 8.6) was added. Protein digestion and peptide elution was performed according to Cerletti et al[18]. The extracted peptides were dried using a SpeedVac and stored at $- 20$ °C. Before MS-analysis peptides were resuspended in 20 μl of buffer A (0.1% formic acid in water, ULC/MS, Biosolve, Netherlands) with 2% (v/v) acetonitrile by sonication for 10 min and transferred to LC-MS grade glass vials (12 × 32 mm glass screw neck vial, Waters, USA). Each measurement was performed with 8 μl of sample.

One-dimensional nLC-ESI-MS/MS

An UPLC HSS T3 column (1.8 μm, 75 μm × 150 mm, Waters, Milford, MA, USA) and an UPLC Symmetry C_{18} trapping column (5 μm, 180 μm × 20 mm, Waters, Milford, MA, USA) for LC as well as a PicoTip Emitter (SilicaTip, 10 μm i.d., New Objective, Woburn, MA, USA) were used in combination with the nanoACQUITY gradient UPLC pump system (Waters, Milford, MA, USA) coupled to a LTQ Orbitrap Elite mass spectrometer (Thermo Fisher Scientific Inc., Waltham, MA, USA). For elution of the peptides a linear gradient with increasing concentration of buffer B (0.1% formic acid in acetonitrile, ULC/MS, Biosolve, Netherlands) from 1% to 40% within 165 min was

applied, followed by a linear gradient from 40% to 99% acetonitrile concentration within 15 min

(0–5 min: 1% buffer B; 5–10 min: 5% buffer B; 10–165 min: 40% buffer B; 165–180 min: 99%

buffer B; 180–195 min: 1% buffer B) at a flow rate of 400 nL min^{-5} and a spray voltage of 1.5–

1.8 kV. The column was re-equilibrated at 1% buffer B within 15 min. The analytical column oven

was set to 55 °C and the heated desolvation capillary was set to 275 °C. The LTQ Orbitrap Elite via

instrument method files of Xcalibur (Rev. 2.1.0) in positive ion mode. The linear ion trap and

Orbitrap were operated in parallel, i.e. during a full MS scan on the Orbitrap in the range of 150–

2,000 *m/z* at a resolution of 240,000 MS/MS spectra of the 20 most intense precursors, from most

intense to least intense, were detected in the ion trap. The relative collision energy for collision-

induced dissociation (CID) was set to 35%. Dynamic exclusion was enabled with a repeat count of

1 and 60 seconds exclusion duration window. Singly charged and ions of unknown charge state

were rejected from MS/MS.

Protein identification and quantification

Protein identification was performed by SEQUEST[26] and MS Amanda[27] algorithms embedded in

Proteome Discoverer 1.4 (Thermo Electron © 2008–2012) searching against the complete proteome

database of *H. volcanii DS2* containing 4035 entries exported from the Halolex database[28] on

9/24/2013. The mass tolerance for precursor ions and fragment ions was set to 6 ppm and 0.4 Da,

respectively. Only tryptic peptides with up to two missed cleavages were accepted. As static peptide

modification the carbamidomethylation of cysteine and as variable peptide modification the

oxidation of methionine as well as the conversion of glutamine (Gln) to pyro-glutamate (pyro-glu)

at any N-terminus were admitted. The false discovery rate (FDR) was determined with the

percolator validation in Proteome Discoverer 1.4 and the q-value was set to 1%[29]. For protein

identification the mass spec format-(msf)-files were filtered with peptide confidence "high" and two

different peptides per protein. Additionally protein grouping options were enabled as default, which

means consider only PSMs (peptide scoring mass spectrum matches), with confidence at least

"medium" and consider only PSMs with delta CN better than 0.15. Proteins were quantified by spectral counting[30, 31] and a protein was considered as significantly regulated at a p value ≤ 0.05 (Student's t-test) and fold ≥ 1.5. Only proteins that had on average at least 5 PSMs were taken into consideration.

Generation of an expression vector of His tagged PrsW

The predicted PrsW protease gene (HVO_0408) was PCR-amplified from *H. volcanii* H26 genomic DNA. The amplicon (1038 bp) was synthesized using primers FWPrsWNcoI (5´ ATATCCATGGACCAGCAGGACCCA 3´) and RvPrsWBamHI (5´ ATATGGATCCTCAGTCCTCGAACTCG 3´) in a reaction mixture containing Phusion GC buffer (1x), 0.2 mM dNTPs, 0.6 mM of each primer 4% (v/v) DMSO and 0.5 units of Phusion DNA polymerase (New England Biolabs) in a final volume of 25 µl. The program used was 98 °C (30 sec), 30 cycles of 98 °C (10 sec)-60 °C (30 sec)-72 °C (30 sec) and a final extension of 72 °C (1 min). The PCR product was cloned in the ZeroBlunt® TOPO cloning vector (ThermoFisher, Inc.). The identity of the amplification product was confirmed by sequencing (Macrogene, Korea). The DNA fragment corresponding to PrsW was excised from the ZeroBlunt® TOPO by digestion with NcoI and BamHI and subcloned with an N- terminal 6x his tag in the *H. volcanii* expression vector pTA963[32]. The ligation product was transformed into *E. coli* DH10β and then passed through *E. coli* GM33 in order to obtain non-methylated DNA and finally, in troduced in *H. volcanii* H26 or MIG1 by the standard PEG method[20].

Protein stability determination

H. volcanii H26 and MIG1 harboring the pTA963-PrsW his tagged construction were grown until they reached a OD_{600} of 0.3-0.5 and then1 mM tryptophan was added and left O/N in order to induce the *ptnaA* promoter. After incubation with tryptophan, 100 µg/ml puromycin was added to the cultures. Samples (5 ml) were taken at the indicated times and membrane fractions were

obtained as detailed above.

Western blotting

Polyacrylamide gels (12% w/v) were transferred to PVDF membranes (80 mA, 2h) and blocked with TBST buffer [25mM Tris-HCl, pH 7.4, 0.01% (v/v) Tween 20)] with 5% (w/v) skimmed milk. Membranes were incubated with 1:5000 anti-His antibody (Biolegend) in blocking buffer, washed with TBST (3 x 10 min), and incubated with 1:10,000 alkaline phosphatase-conjugated anti-mouse IgG (Sigma-Aldrich) for 2 h. After washing (TBST, 3 x 10 min), blots were developed with 0.33 mg/ml nitro blue tetrazolium and 0.01 mg/ml 5-bromo-4-chloro-3-indolyl-phospate.

Cell adhesion assay

Surface adhesion was assessed based on the method described by Tripepi et al[33]. *H. volcanii* cultures (3 ml) at an OD_{600} of ∼0.3 were incubated in 50 ml sterile screw cap plastic tubes. Glass coverslips were inserted into each tube at an angle of 90° and were incubated without shaking. After the indicated time intervals, coverslips were removed with forceps, submerged for 2 min in 2% (v/v) acetic acid and allowed to air dry. Dry coverslips were stained in 0.1% (w/v) crystal violet for 10 min, washed (x3) with distilled water, air dried and then observed by light microscopy using a Nikon Eclipse Ti microscope.

Results and Discussion

Global analysis of total proteins identified in *H. volcanii* wt and Δ*rhoII* (MIG1) strains

In order to investigate the relevance of Rho in *H. volcanii* physiology, the differential proteome

map between the parent (H26) and a mutant strain (MIG1) containing a chromosomal deletion in one of the two Rho homolog genes, *rhoII* (HVO_0727), was assessed. Culture media supernatant, membrane and cytoplasmic proteins obtained from triplicate cultures of both strains harvested in exponential (exp) (OD_{600} 0.5-0.6) and stationary (st) (OD_{600} 1.8-1.9) growth phases were subjected to SDS-PAGE, digested with trypsin and then analyzed by nano-LC-MS/MS as described in the Experimental Section. As Rho exert their proteolytic activity within the membrane environment, their natural substrates are expected to be integral membrane proteins. Thus, in order to analyze the membrane fraction in more detail in search of putative RhoII direct targets, the same assay was repeated only with membrane fractions (triplicates) from *H. volcanii* H26 and MIG1 at exp growth phase.

Out of 4035 total proteins from the predicted *H. volcanii* proteome, 1847 (45.8 %) were identified, including all strains, growth phases and cell fractions of both experiments. The complete list of detected proteins is included in Table S1. From these, 276 (14.9 %) are predicted to be integral membrane proteins, 133 (7.2 %) membrane-associated either by a predicted signal peptide and/or lipobox, and the remaining 1438 (77.8 %) as soluble proteins (Table S1). Figure 1 shows the number of identified proteins distributed according to strain and growth phase (Fig. 1A) and functional category (Fig. 1B). The protease RhoII (HVO_0727) was not detected in membrane fractions of *H. volcanii* H26 (exp and st phase) in none of the two assays. This outcome was not unexpected since integral membrane proteins containing several TMS and/or hydrophobic stretches, such as RhoII are hardly detected by MS technology, as they are underrepresented in trypsin digestion products[34]. However, when these samples were used in a PROTOMAP assay, RhoII was detected in the parental strain but not in the mutant confirming the absence of this protease in MIG1 (see below).
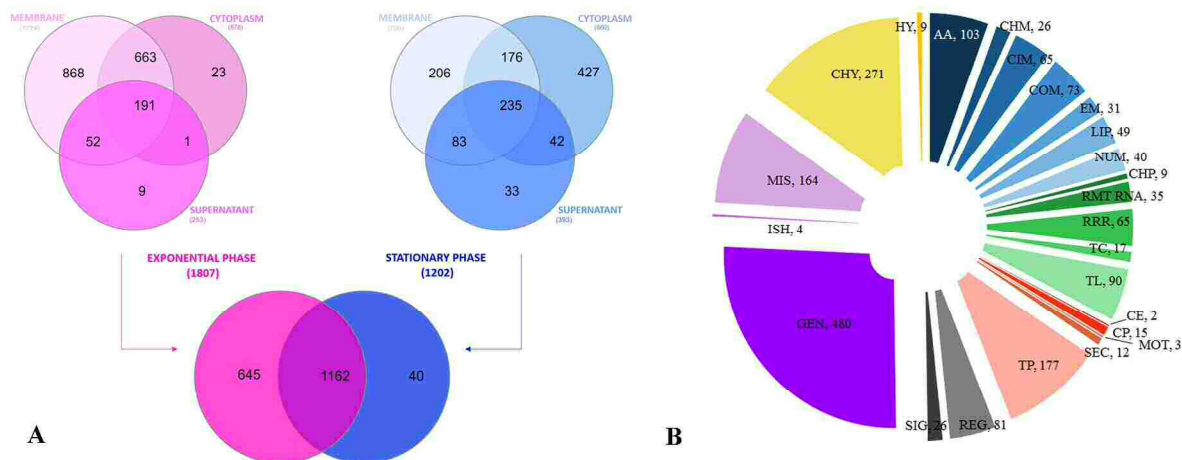
Figure 1. Total identified protein distribution in *H. volcanii* H26 and MIG1 strains. Protein detection was based on a minimum of two different peptides (in at least one biological replicate) with a minimal false discovery rate of q-value ≤ 1%. **A.** Venn diagrams[35] showing the distribution of identified proteins in both strains and growth stages (center) and for each growth stage, the distribution of proteins according to cellular fraction (upper diagrams). **B**. Functional categories corresponding to identified proteins, according to HaloLex Database. **MET** (metabolism, blue): AA amino acid metabolism, CHM carbohydrate metabolism, CIM central intermediary metabolism, COM coenzyme metabolism, EM energy metabolism, LIP lipid metabolism, NUM nucleotide metabolism. **GIP** (genetic information processing, green): CHP chaperones, RMT RNA maturation, RRR replication, repair, recombination, TC transcription, TL translation. **TP_CP** (transport and cellular processes, red): CP cellular processes, SEC protein secretion, MOT motility, TP small molecule transport. **ENV** (environmental information processing, grey): REG gene regulation, SIG signal transduction. **MIS** (miscellaneous functions, purple): GEN general enzymatic function: ISH transposases and ISH-encoded proteins, MIS miscellaneous. **UNASS** (unassigned function, yellow): CHY conserved hypothetical protein, HY hypothetical protein.

Proteins differentially represented in the *H. volcanii* RhoII deficient strain

Using the criteria described in M&M, a total of 103 proteins were differentially represented between the H. volcanii H26 parent and MIG1 strains. Table 1 shows the proteins which evidenced significant variation in amount, organized by growth phase and cellular fraction. Thirty-three proteins (4 from culture medium supernatants, 9 from membrane and 20 from cytoplasm) were enriched while 70 proteins (23 from culture medium supernatant, 32 from membrane and 15 from cytoplasm) decreased their concentration. Most of the proteins that showed variation in their concentration were detected in membrane fractions, in accordance with RhoII exerting its role within the membrane.

The proteins differing between strains in the exp and st growth phases were not coincident, suggesting a growth phase-dependent effect of the rhoII knock-out (Table 1). The impact of the RhoII protease deficiency in cytoplasm and membrane protein samples was more evident in vegetative cells (exp phase) than in non-actively growing cells (st phase), since 60 vs. 16 proteins varied in abundance, respectively. The opposite situation was observed for the secretome fraction in which only 3 proteins were differential (accumulated) in vegetative cells, while 24 varied in concentration (1 increased and 23 decreased) in st phase cultures. It is likely that changes in the cell proteome, produced in absence of rhoII during the exp growth phase, may be reflected on the secretome of the mutant at a later stage of growth. A volcano plot (Fig. 2) was generated in order to visualize the dataset changes obtained in these experiments, by plotting $-\log10$ (p-value) vs. $\log2$ (fold-change) for proteins differentially detected in MIG1 samples taken in exp (Fig. 2A) and st (Fig. 2B) phase of growth. Of those proteins meeting statistically significant criteria (p value ≤ 0.05; fold ≥ 1.5), 63 were detected in exp phase (27 overrepresented, 36 underrepresented) and 40 in st phase (6 enriched, 34 underrepresented).

The differential proteins belonged to several functional classes (Figure 3, Table 1). Even though the

majority of these proteins corresponded to the miscellaneous and general metabolic pathways, proteins involved in translation and solute transport were the most represented, suggesting that these processes are affected by RhoII. However, the growth performance of the mutant was not affected at standard laboratory conditions[17], probably due to a functional overlap between the two Rho homologs present in *H. volcanii*.

In cytoplasm fractions, 35 proteins were differentially represented in the mutant cells. As all Rho substrates identified so far are integral membrane proteins, these differential proteins are probably a consequence of yet unidentified proteolytic and/or gene expression processes regulated by RhoII, representing an indirect/secondary effect of the knock-out mutation.

Differential proteins with predicted TMS that may have been released to the cytoplasm as a consequence of RhoII activity were not identified in the cytoplasm. This observation suggests that, if present, they were either degraded or not detected under the experimental conditions used in this work.

The proteins which showed altered levels in the cytoplasm fractions were very diverse and they could not be associated to a defined route or metabolic pathway.
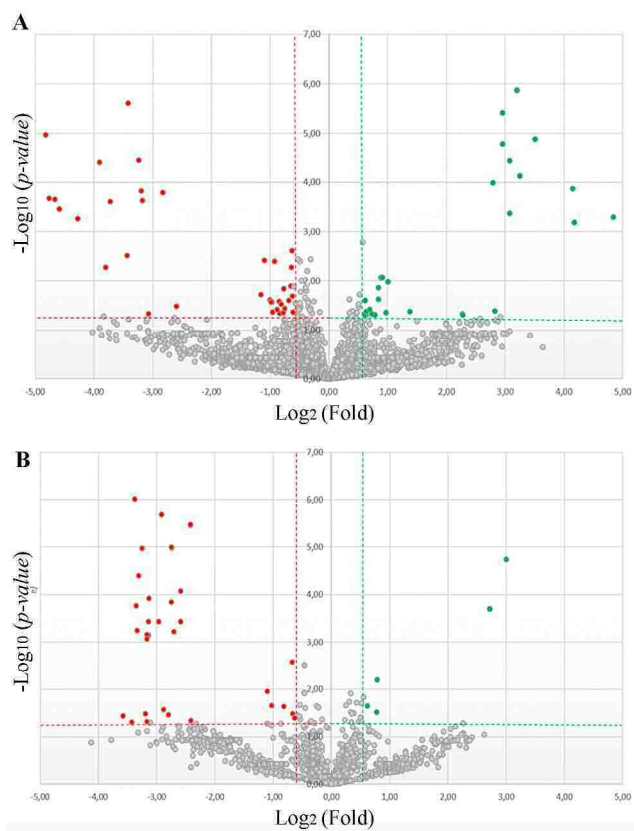
Figure 2. Graphical representation of quantitative proteomics data. Total detected proteins from exp (A) and st (B) growth phases are ranked in a volcano plot according to their statistical p-value ($\log_{10}$) and their relative abundance ratio ($\log_2$ fold change) between MIG1 and H26 strains (x-axis). Off-centered spots are those that vary the most between both groups. Each data point represents a single unique protein identified in our proteomic analysis, color coded as follows: gray indicates no significant change and colored dots indicate significant negative (red) and positive (green) changes.
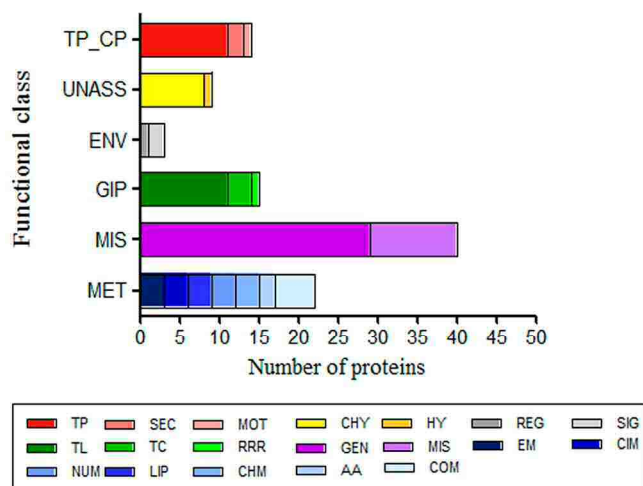
Figure 3. Distribution of the MIG1 differentially expressed proteins into functional classes, according to the Halolex database. For abbreviations, see Fig. 1.

Proteins differentially represented in the membrane fraction (Potential direct targets of RhoII)

A total of 41 proteins were affected by the *rhoII* mutation in membrane fractions (Table 1) comprising 40.2% of the total affected proteins in MIG1. Fourteen proteins detected as differential are predicted to have at least 1 TMS and three (without TMS) contain signal peptides that likely target them to the cell surface. The remaining proteins affected in the mutant may be associated to the membrane via interactions with other molecules (i.e. lipids, other proteins) and likely represent indirect targets of RhoII. For instance, uracil DNA glycosylase (accumulated 28.7 fold in membranes of exponentially growing cells) which participates in DNA base excision repair has been reported to be associated to the mitochondrial inner membrane through electrostatic interactions[36]. Nonetheless, it cannot be discarded that some of these proteins may represent contamination from cytoplasmic origin.

Rho are not processive proteases, therefore, their activity may expose or release a portion of the substrate, leading to changes in size, stability and/or location of the cleaved substrate protein. Consequently, integral membrane proteins which evidenced variations in amount (accumulated or decreased) will be discussed as putative targets of RhoII. Proteins with altered electrophoretic migration were also taken into consideration (see next section).

Rho cleave target proteins within or near a TMS. Most characterized Rho substrates are single TMS, type I or III proteins (N-terminus facing the extracellular side with or without a signal peptide, respectively), even though exceptions are known such as *Drosophila melanogaster* Star, which is a type II membrane protein (N-terminus facing the intracellular side of the cell)[37]. It has been proposed that Rho so far characterized from eukaryotes and bacteria recognize two elements in their natural substrates: part of the TMS and a sequence motif[38].

Among the integral membrane proteins which evidenced differential levels between MIG1 and the parental strain, only HVO_2150, encoding a halocyanin homolog which accumulated in MIG1 (7.8 fold), fulfills the requirements to be a Rho substrate following the criteria proposed by Strisovsky et al.[39] (1TMS, type I or III membrane protein and presence of a 7 amino acid conserved motif).

Halocyanins are blue copper membrane associated proteins from halophilic archaea that are thought to act as mobile electron carriers in a way similar to plant plastocyanins[40]. Cu^{2+} regulates plastocyanin abundance in cyanobacteria, algae and higher plants, which show a decrease in plastocyanin abundance when subjected to Cu deficiency. However, the mechanism of down-regulation varies, as some organisms show Cu-induced variations in mRNA levels while others evidence Cu deficiency-induced plastocyanin proteolysis[41-43]. In *Chlamydomonas*, Cu deficiency-induced proteolysis was proposed to be carried out by the IMP RSEP1 based in gene expression studies[42]. Halocyanin was purified from the haloalkaliphilic archaeon *Natronobacterium pharaonis* and the gene was cloned and sequenced[44], however regulation of halocyanin levels by Cu has not

been confirmed in haloarchaea.

In *Arabidopsis sp.*, mutations in two P-type ATPases (PAA1 and PAA2) that deliver Cu to the chloroplast and thylakoid lumen caused 80–90% reduction of plastocyanin abundance[45, 46]. While plant chloroplast P-type ATPases import Cu to the chloroplast lumen, prokaryotic P-type ATPases contribute to Cu detoxification by copper efflux out of the cell[47]. In the thermophilic and thermoacidophilic archaea *Archaeoglobus fulgidus* and *Sulfolobus solfataricus* CopA ATPases are active Cu export pumps that confer Cu and Ag tolerance[48, 49]. In this study, a P-type ATPase (*copA*, HVO_1751) showed a 2.1 fold reduction in abundance in the MIG1 strain (Table 1). A functional link between halocyanin and the CopA homolog in *H. volcanii* could be hypothesized. Whether RhoII regulates directly halocyanin concentration through processing or indirectly (i.e. by processing of a P-type ATPase and therefore regulating Cu and halocyanin levels) remains to be determined and is focus of future research.

Escherichia coli rhomboid GlpG was shown to cleave heterologous multi pass membrane proteins[13] and the rhomboid protease 1 (RHBDD1) was reported to cleave the 6 TMS TSAP6 protein in human cell lines, allowing for a probably TSAP6-dependent regulation of exosome trafficking[50]. Therefore, in addition to halocyanin, the polytopic integral membrane proteins which evidenced variations in their abundance in MIG1 were also considered as putative RhoII substrates.

Changes in the concentration of proteins involved in regulation of gene expression may explain differences in amount of the protein products of the genes they control. Two polytopic membrane sensor histidine kinases (HVO_0570 and HVO_B0273) were less abundant in MIG1 exp phase samples (Table 1) with negative folds of 1.5 and 13.9, respectively and may represent RhoII direct targets. It has been reported that the Rho PARL mediates cleavage of the histidine kinase PINK1 in the mitochondrial inner membrane, which regulates the activity of respiratory complex

I and the clearance of damaged mitochondria by mitophagy[51].

Four integral membrane metalloproteases showed lower protein levels in MIG1 than in the parental strain (Table 1): peptidase T homolog (HVO_0477, 13.1 fold), Abi/CAAX protease (HVO_1997, 10.7 fold), HtpX- like protease (HVO_A0045, 1.6 fold) and PrsW protease homolog (HVO_0408, 28.2 fold), suggesting that metal-dependent proteolysis at the membrane level is, by some means, regulated by RhoII. This pattern may reflect a specific effect of RhoII on individual proteases but may also be a consequence of altered metal availability caused by variations in metal transporters (Table 1). It is likely that some proteins observed as stabilized in the mutant (Table 1) may accumulate as a consequence of the level reduction of these proteases. To the best of our knowledge, these enzymes have not been characterized in Achaea, and the fact that in this study they were detected at the protein level suggests that they are functional enzymes in *H. volcanii*.

In *Bacillus subtilis* the PrsW peptidase inactivates the anti-sigma factor RsiW by performing the first of several proteolytic cleavages, resulting in the transcription of genes controlled by the extra cytoplasmic function sigma factor σW[52]. To validate the results obtained in the proteomic approach, the *in vivo* stability of the *H. volcanii* PrsW protease was compared in the parental and MIG1 strains. Expression of the *prsW* gene, cloned with an N-terminal His tag downstream the *H. volcanii* tryptophanase promoter (*ptnA*), was induced in both strains by addition of tryptophan (1mM) to the growth medium. Cells were treated with puromycin to block protein translation and the stability of PrsW over time was assessed by Western blotting. While PrsW electrophoretic mobility was not affected in the mutant, the levels of PrsW were significantly reduced after 16 h (Fig. 4), compared to the parental strain. This result correlates with the reduced PrsW levels observed in the mutant in the proteomic approach and suggest that PrsW is affected by RhoII, likely through a proteolytic signaling cascade at the membrane in *H. volcanii* cells. Alternatively, as the

recombinant protein bears an N-terminal 6His tag, processing by RhoII of a small peptide

from the C-terminus (not detected as a shift in migration in the SDS-PAGE) may increase

the stability of PrsW in the parental strain. As the biological function of PrsW in archaea is

not known, at present it is not possible to correlate/evaluate to what extent the deficiency in

PrsW affects the physiology of the *H. volcanii* MIG1 mutant.
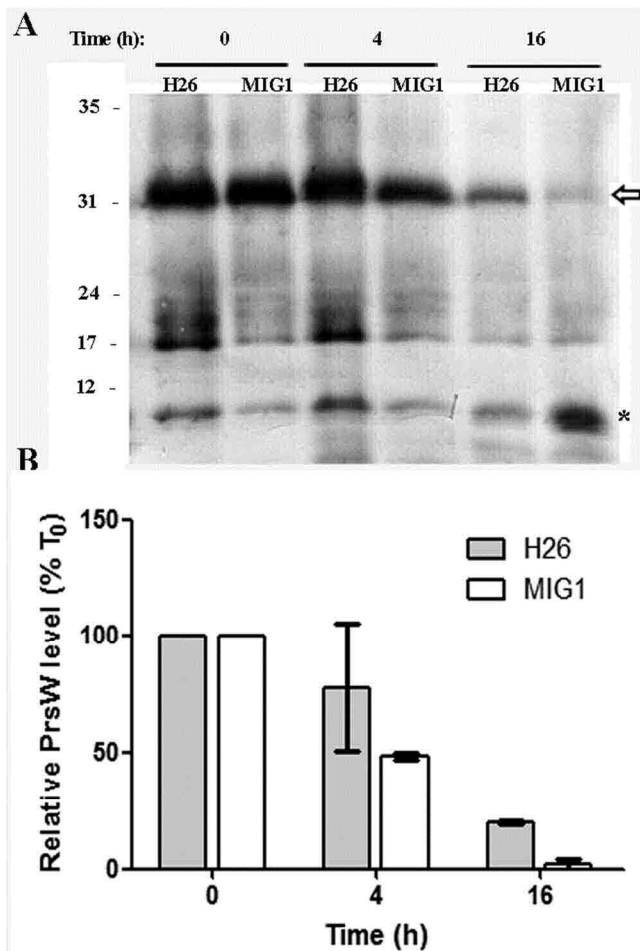
Figure 4. Stability of PrsW homolog in MIG1 strain. *H. volcanii* H26 and MIG1 cells harboring

plasmid pTA963 containing the *prsW* gene with a 6x histidine tag under the *ptn*A promoter were

grown to exp phase in presence of tryptophan 1 mM. At that point puromycin (100 μg//ml) was

added and samples were taken at the indicated times and subjected to SDS-PAGE followed by

western blotting with anti his tag antibody (A). Position of Molecular weight markers (kDa) is

indicated at the left. The arrow points the band corresponding to PrsW and the asterisk a degradation product. The band corresponding to PrsW was quantified with ImageJ (B). The plotted data correspond to two independent experiments. Error bars, S.D.

Proteins differentially represented in the secretome of *H. volcanii*

The growth medium of *H. volcanii* MIG1 (exp plus st phases) showed 27 proteins with variations in their level, compared to the wt (Table 1). Out of these, 8 are predicted secretory proteins, 4 are expected to be membrane associated via at least 1 TMS, and the remaining are likely soluble proteins. The presence of proteins without a predicted signal peptide in culture medium supernatant is not uncommon; actually, evidence from proteomics studies suggests that there are significant differences between predicted and experimental archaeal secretomes[53, 54]. These differences may be due to unconventional secretion such as vesicle transport, or a consequence of cell lysis. In any case, soluble proteins (with or without a signal peptide) which displayed differences in their levels in MIG1 supernatants may represent an indirect effect of the *rhoII* deletion.

Four integral membrane proteins were underrepresented in MIG1 culture media supernatants (Table 1). Out of these, SecD (HVO_1976), flagellin 1 (HVO_1210) and signal peptidase I (HVO_2603) were detected in both strains while the conserved hypothetical protein (HVO_1153)] was not detected in the supernatants of MIG1 cultures. The absence of peptides from HVO_1153 in the culture medium supernatant of MIG1 could be a consequence of the lack of processing by RhoII.

SecD and Sec1a are proteins involved in the Sec protein translocation pathway [55, 56]. Even though they were both affected in the mutant, the proteomic data did not provide additional evidence suggesting that this pathway is altered in MIG1.

HVO_1153 is a conserved hypothetical protein with 1 TMS. BLAST searches indicated that this

protein has homology with archaeal flagellin domain-containing proteins and also with bacterial adhesins, and thus the lack of processing of HVO_1153 in MIG1 may contribute to the observed defects in motility and cell adhesion (see below) previously evidenced in the mutant. Amino acid sequence analysis with Pattinprot (https://npsa-prabi.ibcp.fr/cgi-bin/pattern_pattinprot.pl) evidenced the presence of a Rho consensus motif within the predicted TMS of this hypothetical protein. Thus it can be hypothesized that the presence of peptides from HVO_1153 in the culture medium of the wt strain may be due to RhoII proteolytic activity.

Flagellin 1 is the major component of the *H. volcanii* flagellum and deletion of the corresponding gene, *flgA1*, renders non motile cells[33]. Flagella are released from the cell surface through centrifugation, therefore, the reduced level of flagellin peptides in the culture supernatant of MIG1 suggests that flagella are either less abundant and/or not properly assembled which may contribute with the reduced motility reported previously for this mutant[17]. Maturation of flagellin involves N-glycosylation and cleavage by PibD signal peptidase III prior to flagellum assembly[33]. Whether the role of RhoII regulating the level of flagellin in the culture medium is direct or indirect (i. e regulating flagellin glycosylation and flagellum assembly) needs to be experimentally determined. This also applies to Sec11a and HVO_1153, as both have predicted glycosylation sites, according to NetNGlyc server[57].

Identification of proteins with differential migration in the *H. volcanii* *rhoII* KO mutant

Rho cleave their substrates at specific sites releasing peptides which often play a regulatory role[58]. Therefore, to detect variations in the electrophoretic migration of individual proteins that may arise from differential processing in the mutant vs. wt strain, a simplified PROTOMAP assay was

performed[23]. The results are shown in Table 2.

In this assay RhoII (HVO_0727) was detected in membranes from the parental strain while it was not evidenced in MIG1, confirming the absence of the RhoII protease in this mutant. This finding agreed with the observation that a higher percentage of total proteins with predicted TMS were detected in this experiment compared to the previous analysis (21 *vs.* 12%, respectively) (Tables S1 and S3).

A total of 99 proteins showed differences in amount (fold $\geq$ 1.5) in at least one of the gel sections (Table 2). Twenty-one (21) integral membrane proteins displayed differences comparing the mutant vs. wt strain and may represent a direct consequence of RhoII proteolytic activity (absence/presence). In addition, 78 predicted soluble proteins showed differential migration in the PROTOMAP experiment. These probably represent proteins that were secondarily/indirectly affected by the *rhoII* deletion, as a consequence of absence of processing by other protease/s or by another altered posttranslational modification process.

Several proteins involved in solute transport across cell membranes showed altered electrophoretic migration including 16 ABC transporter components for lipoproteins, peptides, Zn^{2+}, cobalamin, phosphate and sugars (Table 2). In addition, three integral membrane metal transporters (probable Zn/Cd transport protein-HVO_2602 and P-type ATPase-HVO_1751, Mg transport protein CorA-HVO_1675) displayed altered migration with negative folds of 8.4 (section 3), 1.7 (section 3) and 5.2 (section 2), respectively. P-type ATPase also showed reduced levels in quantitative proteomics experiment (see above). It is possible that differences in metal ion availability would in turn cause to some extent variations in other metalloprotein levels (i.e. metalloproteases, see above). Metal ions have a key role in the physiology of cells, as they act as the redox centers for metalloproteins such as cytochromes, blue copper proteins, and iron-sulfur proteins which play a vital role in electron transport. On the other hand, any disturbance in metal ion homeostasis could produce toxic

effects on cell viability. Among *Archaea*, thermophiles, hyperthermophiles and methanogens utilize P-type ATPases and ABC transporters for metal transport and balancing. However, metal homeostasis in haloarchaea has not been extensively studied[59]. Independently if the observed difference in concentration of metal transporter proteins is a direct or indirect effect of RholI absence, these data, together with the semi quantitative proteomics results (Table 1) suggest that metal homeostasis is affected in MIG1. However, under standard laboratory conditions, this effect was not reflected in cell proliferation and growth.

Proteins with differential migration related to the phenotypes of the MIG1 strain

Soluble proteins

DNA gyrase is an essential bacterial enzyme that catalyzes the ATP-dependent negative super-coiling of double-stranded closed circular DNA. Gyrase is a topoisomerase involved in the control of topological transitions of DNA[60]. The active form of this enzyme is a tetramer of two A and two B subunits[61]. Novobiocin is a DNA gyrase inhibitor that binds to the active enzyme[62]. In this work we observed that the DNA gyrase subunit A was reduced by about 2 fold in section 2 of the PROTOMAP gel (Table 2). The abnormal migration of subunit A in the *rhoII* mutant suggests that migration of this polypeptide is altered (i.e. affected by post translational modification) generating a DNA gyrase more susceptible to novobiocin inhibition that could account for the enhanced sensitivity to novobiocin displayed by the MIG1 strain[17].

In *H. volcanii*, the *rhoII* gene is part of an operon with the sequence encoding EndV (HVO_0726), an endonuclease involved in DNA repair in *E. coli*[63]. We have shown that *endV* mRNA is expressed in *H. volcanii* H26 and MIG1 at similar levels[17]. MIG1 cells irradiated with UV light in liquid

minimal medium cultures, showed a delay in resuming growth when compared to the wt (Figure S2), evidencing that the mutant has difficulty in coping with UV stress. In this study, the soluble protein RadA (HVO_0104) which is involved in DNA repair after UV irradiation[64] was reduced by 1.9 fold in section 2 in the mutant (Table 2). Even though the functional link between RhoII, EndV and RadA remains to be addressed, our data suggest that RhoII may participate in the regulation of DNA repair processes in *H. volcanii.* A link between UV irradiation and Rho has been reported for RHBDL2 which showed upregulation upon UV treatment in human keratynocites[65].

Integral membrane proteins

H. volcanii is surrounded by a hexagonally packed surface S-layer, formed by the SLG. This glycoprotein contains 7 predicted N-glycosylation sites. Out of these, N83, N13, N274 and N279 are decorated with a pentasaccharide which also occurs in *H. volcanii* flagellins and pilins[65-67]. In addition, position N498 is decorated with a tetrasaccharide synthesized only in low salt growth conditions[68]. Our previous work showed that N-732 in the SLG harbors a novel sulfoquinovose containing oligosaccharide (GlcNAc-GlcNAc(Hex)$_2$-(SQ-Hex)$_6$) which is truncated in the MIG1 strain[17].

Several enzymes potentially involved in protein glycosylation were detected as differential by shotgun proteomics (Table 1) and in the PROTOMAP experiment (Table 2). A list along with their proposed/known roles is provided in Table S2. Agl15 (HVO_2050), a flippase which participates in the synthesis of low salt tetrasaccharide at position N498 of SLG[67], was the only affected glycosylase predicted to be an integral membrane protein (14 TMS) with an 8.1 fold reduction at section 3 of the PROTOMAP. Whether this protein is involved in the N-732 glycosylation of SLG is not known. However, if this were the case, Agl15 processing/activation by RhoII may account at least in part for the differences in SLG glycosylation observed in the mutant[17]. Alternatively, it is

also possible that RhoII cleaves an unknown substrate that regulates the level of one or more of these glycosylation enzyme/s (Table S2) leading to an abnormal glycosylation pattern of the SLG.

SLG is initially synthesized with a C-terminal transmembrane domain and following proteolytic cleavage upstream of the TMS, the truncated protein is transferred to a lipid anchor[69]. The involvement of the ArtA archaeosortase in the proteolytic processing of the C-terminus of this glycoprotein was reported by Abdul Halim et al[70]. In this study SLG was enriched 1.5 fold in section 2 and 1.7 fold in section 3 of the PROTOMAP (Table 2). The differential electrophoretic migration of this protein may be due to the previously observed truncation of the oligosaccharide bound to N732 in the mutant strain. However, it cannot be ruled out that RhoII may also contribute to proteolytic processing of SLG.

The preflagellin peptidase PibD was reduced 7.7 fold in section 3 and evidenced a 2 fold reduction in level when calculating the total fold (Table 2), indicating that its electrophoretic migration was altered but also that the protein concentration was lower in MIG1 cells. PibD is known to process preflagellins and prepilins prior to flagella and pili assembly in archaea[71]. It was shown that a knock-out mutation of *pibD* abolished swimming motility and adhesion to glass surfaces in *H. volcanii*[33]. Therefore, decreased amounts of PibD in MIG1 cells may explain the reduced motility of this strain in soft agar plates[17]. In order to determine whether cell adhesion was also affected in the MIG1 mutant, we examined the ability of these cells to adhere to glass slides. As observed in Fig. 5, the Rho mutant showed reduced adhesion to glass plates compared to the parental strain. In addition, PilA1 (HVO_0972), a substrate of PibD[71], was accumulated in section 4 of the gel. It could be proposed that RhoII is involved in proteolytic maturation/processing of PibD affecting pilin (and probably flagellin, see Table 1) processing and/or assembly and therefore *H. volcanii* motility.
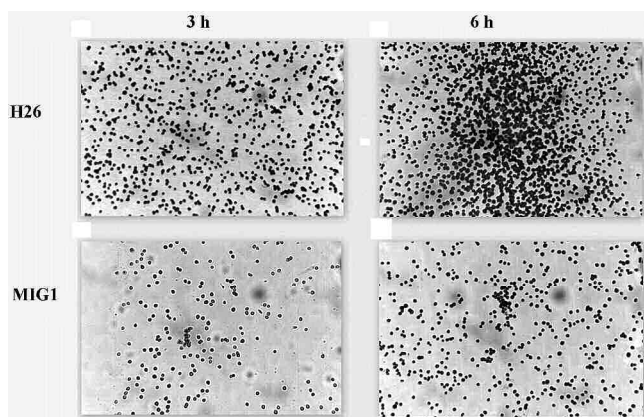
Figure 5. Cells from *H. volcanii* MIG1 strain show reduced adhesion to glass surfaces. Adhesion to glass coverslips was tested using a previously described protocol[33]. Coverslips were placed in 50 ml plastic tubes, containing 6 ml of MGM 18% medium cultures of *H. volcanii* H26 and MIG1 at an OD_{600} of 0.3. After 3 or 6 h incubation at 42 °C, cells were fixed with 2% acetic acid, stained with 0.1% crystal violet and observed by light microscopy. Light micrographs of the coverslips were taken at 100x magnification.

Analysis of semi-tryptic peptides in integral membrane proteins

Detection of proteins with different levels and/or electrophoretic mobility variations was performed against a trypsin digestion database. In order to identify peptides that may result from RhoII proteolytic activity, a search of semi-tryptic peptides was also performed. This analysis focused on proteins with semi-tryptic peptide/s (found exclusively in the wt) inside or near a TMS and which evidenced a Rho cleavage motif (Table S4). A total of 10 candidates were identified in all the experiments performed, including PibD, hypothetical proteins and small solute transporters. However, it has to be noted that it is not known whether archaeal rhomboid proteases recognize the same cleavage motif as their bacterial and eukaryotic counterparts. Experimental validation and cleavage site identification of *H. volcanii* RhoII predicted substrates will contribute to clarify this

Concluding remarks

This study shows for the first time, the effect of a rhomboid protease gene deletion on the proteome of an archaeon. Previous studies have examined the influence of Rho deficiency on specific subproteomes, such as *A. thaliana* chloroplasts[72] and the secretome of *Trichomonas vaginalis*[73], however, our study focused on a more comprehensive analysis of the relevance of Rho at the whole proteome level.

Elimination of *rhoII* from *H. volcanii* chromosome had a global impact on the proteome, affecting soluble, membrane-associated as well as secreted proteins with diverse biological functions, suggesting a role for this protease in the regulation of processes such as solute transport, Cu homeostasis, signal transduction, protein glycosylation, cell adhesion and motility. Interestingly, some of these proteins are associated with the differential phenotypes observed in the *rhoII* mutant. A schematic representation of the proteins showing differences in their levels and/or electrophoretic migration and their involvement in the generation of the mutant phenotypes is provided in Fig. 6. Ongoing work is focused on the validation of selected candidate substrates of RhoII which will contribute to get insight on the biological function of this family of IMPs in the *Archaea* domain.

Figure 6. Schematic representation of the effect of deleting *rhoII* in *H. volcanii* physiology. Elimination of *rhoII* from the chromosome causes several phenotypes in *H. volcanii* cells. Proteins that showed variations in level and/or electrophoretic mobility in this work and that are potentially involved in the generation of these phenotypes are listed in the corresponding box. Blue font denotes proteins that showed differential migration in the PROTOMAP assay. The arrows indicate proteins with augmented (green) or decreased concentration (red) in the mutant. The proposed role of RhoII in the processing of the conserved hypothetical protein HVO_1153 and PibD (affecting cell adhesion and motility) is detailed on the right.

1
2
3
4
5
6
7
8
9
10
11
12
13
14
15
16
17
18
19
20
21
22
23
24
25
26
27
28
29
30
31
32
33
34
35
36
37
38
39
40
41
42
43
44
45
46
47
48
49
50
51
52
53
54
55
56
57
58
59
60

Supporting information

Figure S1. Cartoon representation of SDS gels used for comparative quantitative proteomics or for

the simplified PROTOMAP assay sample preparation.

Figure S2. Effect of UV irradiation on *H. volcanii* MIG1 growth.

Table S1. Proteins detected in (membrane, cytoplasm and cell culture supernatants) of *H. volcanii*

H26 and MIG1 at exp and st phase of growth

Table S2. Proteins involved in N-glycosylation with affected level and/or migration in MIG1. CE:

cytoplasm of exp phase. ME: membrane fraction of exp phase.

Table S3. Proteins detected in membranes of exponentially growing H26 and MIG1 strains in the

PROTOMAP assay.

Table S4. Semitryptic peptides with a rhomboid cleavage consensus detected in membrane proteins.

The authors declare no competing financial interest.

AUTHOR INFORMATION

Corresponding authors

* María I. Giménez. Email: migimen@mdp.edu.ar. Tel: 54-223-4753030 int 12.

* Ansgar Poestch. Email: ansgar.poetsch@rub.de.

ABBREVIATIONS

Rho, rhomboid proteases; IMP, intramembrane protease; TMS, transmembrane segment; exp, exponential; st, stationary; nLC-ESI-MS/MS, Nano-scale liquid chromatographic electrospray ionization tandem mass spectrometry; SLG, S-layer glycoprotein.

REFERENCES

1.   Lopez-Otin, C.; Overall, C. M., Protease degradomics: a new challenge for proteomics. *Nature reviews. Molecular cell biology* **2002,** *3* (7), 509-19.

2.   Gimenez, M. I.; Cerletti, M.; De Castro, R. E., Archaeal membrane-associated proteases: insights on Haloferax volcanii and other haloarchaea. *Frontiers in microbiology* **2015,** *6*, 39.

3.   Verhelst, S. H., Intramembrane proteases as drug targets. *The FEBS journal* **2017, 284(10), 1489-1502**.

4.   Freeman, M., The rhomboid-like superfamily: molecular mechanisms and biological roles.

Annual review of cell and developmental biology **2014,** *30*, 235-54.

5.   Lee, J. R.; Urban, S.; Garvey, C. F.; Freeman, M., Regulated intracellular ligand transport

and proteolysis control EGF signal activation in Drosophila. *Cell* **2001,** *107* (2), 161-71.

6.   Urban, S.; Lee, J. R.; Freeman, M., A family of Rhomboid intramembrane proteases

activates all Drosophila membrane-tethered EGF ligands. *The EMBO journal* **2002,** *21* (16), 4277-

86.

7.   Spinazzi, M.; De Strooper, B., PARL: The mitochondrial rhomboid protease. *Seminars in cell*

& developmental biology **2016,** *60*, 19-28.

8.   Sibley, L. D., The roles of intramembrane proteases in protozoan parasites. *Biochimica et*

biophysica acta **2013,** *1828* (12), 2908-15.

9.   Dhingra, S.; Kowlaski, C. H.; Thammahong, A.; Beattie, S. R.; Bultman, K. M.; Cramer, R. A.,

RbdB, a Rhomboid Protease Critical for SREBP Activation and Virulence in Aspergillus fumigatus.

mSphere **2016,** *1* (2), e00035-16.

10.   Stevenson, L. G.; Strisovsky, K.; Clemmer, K. M.; Bhatt, S.; Freeman, M.; Rather, P. N.,

Rhomboid protease AarA mediates quorum-sensing in Providencia stuartii by activating TatA of

the twin-arginine translocase. *Proceedings of the National Academy of Sciences of the United*

States of America **2007,** *104* (3), 1003-8.

11.   Akiyama, Y.; Maegawa, S., Sequence features of substrates required for cleavage by GlpG,

an Escherichia coli rhomboid protease. *Molecular microbiology* **2007,** *64* (4), 1028-37.

12.   Maegawa, S.; Ito, K.; Akiyama, Y., Proteolytic action of GlpG, a rhomboid protease in the

Escherichia coli cytoplasmic membrane. *Biochemistry* **2005,** *44* (41), 13543-52.

13.   Erez, E.; Bibi, E., Cleavage of a multispanning membrane protein by an intramembrane

serine protease. *Biochemistry* **2009,** *48* (51), 12314-22.

14.   Mesak, L. R.; Mesak, F. M.; Dahl, M. K., Expression of a novel gene, gluP, is essential for

normal Bacillus subtilis cell division and contributes to glucose export. *BMC microbiology* **2004,** *4*,

13.

15.   Kateete, D. P.; Katabazi, F. A.; Okeng, A.; Okee, M.; Musinguzi, C.; Asiimwe, B. B.; Kyobe, S.;

Asiimwe, J.; Boom, W. H.; Joloba, M. L., Rhomboids of Mycobacteria: characterization using an

aarA mutant of Providencia stuartii and gene deletion in Mycobacterium smegmatis. *PloS one*

2012, *7* (9), e45741.

16.   Kinch, L. N.; Grishin, N. V., Bioinformatics perspective on rhomboid intramembrane

protease evolution and function. *Biochimica et biophysica acta* **2013,** *1828* (12), 2937-43.

17.   Parente, J.; Casabuono, A.; Ferrari, M. C.; Paggi, R. A.; De Castro, R. E.; Couto, A. S.;

Giménez, M. I., A rhomboid protease gene deletion affects a novel oligosaccharide N-linked to the

S-layer glycoprotein of Haloferax volcanii. *The Journal of biological chemistry* **2014,** *289* (16),

11304-17.

18.   Cerletti, M.; Paggi, R. A.; Guevara, C. R.; Poetsch, A.; De Castro, R. E., Global role of the

membrane protease LonB in Archaea: Potential protease targets revealed by quantitative

proteome analysis of a lonB mutant in Haloferax volcanii. *Journal of proteomics* **2015,** *121*, 1-14.

19.   Nieuwlandt, D. T., Palmer, J. R., Armbruster, D. T., Kuo, Y. P., Oda, W. and Daniels, C. J., In

Archaea: A Laboratory Manual, Robb, F. T., Place, A. R., Sowers, K. R., Schreier, H. J., DasSarma, S.

and Fleischmann, E. M.,, Ed. Cold Spring Harbor Laboratory Press: Cold Spring Harbor, NY, 1995; pp

161-162.

20.   Dyall-Smith, M., The halohandbook. *Protocols for haloarchaeal genetics. Edited by: Dyall-*

Smith M. University of Melbourne **2009,** *144 pp*.

http://www.haloarchaea.com/resources/halohandbook/

21.   Sambrook, J.; Russell, D. W., Molecular cloning: a laboratory manual. *Cold Spring Harbor*

Laboratory Press, Cold Spring Harbor, NY **2001**.

22.   Laemmli, U. K., Cleavage of structural proteins during the assembly of the head of

bacteriophage T4. *Nature* **1970,** *227* (5259), 680-5.

23.   Dix, M. M.; Simon, G. M.; Cravatt, B. F., Global identification of caspase substrates using

PROTOMAP (protein topography and migration analysis platform). *Methods in molecular biology*

2014, *1133*, 61-70.

24.   Candiano, G.; Bruschi, M.; Musante, L.; Santucci, L.; Ghiggeri, G. M.; Carnemolla, B.;

Orecchia, P.; Zardi, L.; Righetti, P. G., Blue silver: a very sensitive colloidal Coomassie G-250

staining for proteome analysis. *Electrophoresis* **2004,** *25* (9), 1327-33.

25.   Schluesener, D.; Fischer, F.; Kruip, J.; Rogner, M.; Poetsch, A., Mapping the membrane

proteome of Corynebacterium glutamicum. *Proteomics* **2005,** *5* (5), 1317-30.

26.   Eng, J. K.; McCormack, A. L.; Yates, J. R., An approach to correlate tandem mass spectral

data of peptides with amino acid sequences in a protein database. *Journal of the American Society*

for Mass Spectrometry **1994,** *5* (11), 976-989.

27.   Dorfer, V.; Pichler, P.; Stranzl, T.; Stadlmann, J.; Taus, T.; Winkler, S.; Mechtler, K., MS

Amanda, a universal identification algorithm optimized for high accuracy tandem mass spectra.

Journal of proteome research **2014,** *13* (8), 3679-84.

28.   Pfeiffer, F.; Broicher, A.; Gillich, T.; Klee, K.; Mejia, J.; Rampp, M.; Oesterhelt, D., Genome

information management and integrated data analysis with HaloLex. *Archives of microbiology*

2008, *190* (3), 281-99.

29.   Kall, L.; Storey, J. D.; MacCoss, M. J.; Noble, W. S., Posterior error probabilities and false

discovery rates: two sides of the same coin. *Journal of proteome research* **2008,** *7* (1), 40-4.

30.   Liu, H.; Sadygov, R. G.; Yates, J. R., 3rd, A model for random sampling and estimation of

relative protein abundance in shotgun proteomics. *Analytical chemistry* **2004,** *76* (14), 4193-201.

31.   Haussmann, U.; Qi, S. W.; Wolters, D.; Rogner, M.; Liu, S. J.; Poetsch, A., Physiological

adaptation of Corynebacterium glutamicum to benzoate as alternative carbon source - a

membrane proteome-centric view. *Proteomics* **2009,** *9* (14), 3635-51.

32.   Allers, T.; Barak, S.; Liddell, S.; Wardell, K.; Mevarech, M., Improved strains and plasmid

vectors for conditional overexpression of His-tagged proteins in Haloferax volcanii. *Applied and*

environmental microbiology **2010,** *76* (6), 1759-69.

33.   Tripepi, M.; Imam, S.; Pohlschroder, M., Haloferax volcanii flagella are required for motility

but are not involved in PibD-dependent surface adhesion. *Journal of bacteriology* **2010,** *192* (12),

3093-102.

34.   Fischer, F.; Poetsch, A., Protein cleavage strategies for an improved analysis of the
membrane proteome. *Proteome science* **2006,** *4*, 2.

35.   Heberle, H.; Meirelles, G. V.; da Silva, F. R.; Telles, G. P.; Minghim, R., InteractiVenn: a web-based tool for the analysis of sets through Venn diagrams. BMC Bioinformatics 2015, 16:169.

36.   Stuart, J. A.; Mayard, S.; Hashiguchi, K.; Souza-Pinto, N. C.; Bohr, V. A., Localization of mitochondrial DNA base excision repair to an inner membrane-associated particulate fraction. *Nucleic acids research* **2005,** *33* (12), 3722-32.

37.   Tsruya, R.; Wojtalla, A.; Carmon, S.; Yogev, S.; Reich, A.; Bibi, E.; Merdes, G.; Schejter, E.; Shilo, B. Z., Rhomboid cleaves Star to regulate the levels of secreted Spitz. *The EMBO journal* **2007,** *26* (5), 1211-20.

38.   Strisovsky, K., Structural and mechanistic principles of intramembrane proteolysis--lessons from rhomboids. *The FEBS journal* **2013,** *280* (7), 1579-603.

39.   Strisovsky, K.; Sharpe, H. J.; Freeman, M., Sequence-specific intramembrane proteolysis: identification of a recognition motif in rhomboid substrates. *Molecular cell* **2009,** *36* (6), 1048-59.

40.   Scharf, B.; Engelhard, M., Halocyanin, an archaebacterial blue copper protein (type I) from Natronobacterium pharaonis. *Biochemistry* **1993,** *32* (47), 12894-900.

41.   Zhang, L.; McSpadden, B.; Pakrasi, H. B.; Whitmarsh, J., Copper-mediated regulation of cytochrome c553 and plastocyanin in the cyanobacterium Synechocystis 6803. *The Journal of biological chemistry* **1992,** *267* (27), 19054-9.

42.   Kropat, J.; Gallaher, S. D.; Urzica, E. I.; Nakamoto, S. S.; Strenkert, D.; Tottey, S.; Mason, A. Z.; Merchant, S. S., Copper economy in Chlamydomonas: prioritized allocation and reallocation of copper to respiration vs. photosynthesis. *Proceedings of the National Academy of Sciences of the United States of America* **2015,** *112* (9), 2644-51.

43. Abdel-Ghany, S. E.; Pilon, M., MicroRNA-mediated systemic down-regulation of copper

protein expression in response to low copper availability in Arabidopsis. *The Journal of biological*

chemistry **2008,** *283* (23), 15932-45.

44. Mattar, S.; Scharf, B.; Kent, S. B.; Rodewald, K.; Oesterhelt, D.; Engelhard, M., The primary

structure of halocyanin, an archaeal blue copper protein, predicts a lipid anchor for membrane

fixation. *The Journal of biological chemistry* **1994,** *269* (21), 14939-45.

45. Shikanai, T.; Muller-Moule, P.; Munekage, Y.; Niyogi, K. K.; Pilon, M., PAA1, a P-type

ATPase of Arabidopsis, functions in copper transport in chloroplasts. *The Plant cell* **2003,** *15* (6),

1333-46.

46. Abdel-Ghany, S. E.; Muller-Moule, P.; Niyogi, K. K.; Pilon, M.; Shikanai, T., Two P-type

ATPases are required for copper delivery in Arabidopsis thaliana chloroplasts. *The Plant cell* **2005,**

17 (4), 1233-51.

47. Migocka, M., Copper-transporting ATPases: The evolutionarily conserved machineries for

balancing copper in living systems. *IUBMB life* **2015,** *67* (10), 737-45.

48. Arguello, J. M., Identification of ion-selectivity determinants in heavy-metal transport P1B-

type ATPases. *The Journal of membrane biology* **2003,** *195* (2), 93-108.

49. Völlmecke, C.; Drees, S. L.; Reimann, J.; Albers, S.-V.; Lübben, M., The ATPases CopA and

CopB both contribute to copper resistance of the thermoacidophilic archaeon Sulfolobus

solfataricus. *Microbiology* **2012,** *158* (6), 1622-1633.

50. Wan, C.; Fu, J.; Wang, Y.; Miao, S.; Song, W.; Wang, L., Exosome-related multi-pass

transmembrane protein TSAP6 is a target of rhomboid protease RHBDD1-induced proteolysis. *PloS*

one **2012,** *7* (5), e37452.

51.   Wai, T.; Saita, S.; Nolte, H.; Muller, S.; Konig, T.; Richter-Dennerlein, R.; Sprenger, H. G.;

Madrenas, J.; Muhlmeister, M.; Brandt, U.; Kruger, M.; Langer, T., The membrane scaffold SLP2

anchors a proteolytic hub in mitochondria containing PARL and the i-AAA protease YME1L. *EMBO*

reports **2016,** *17* (12), 1844-1856.

52.   Heinrich, J.; Hein, K.; Wiegert, T., Two proteolytic modules are involved in regulated

intramembrane proteolysis of Bacillus subtilis RsiW. *Molecular microbiology* **2009,** *74* (6), 1412-26.

53.   Ellen, A. F.; Zolghadr, B.; Driessen, A. M.; Albers, S.-V., Shaping the archaeal cell

envelope. *Archaea* **2010,** 608243, 13 pp.

54.   Feng, J.; Wang, J.; Zhang, Y.; Du, X.; Xu, Z.; Wu, Y.; Tang, W.; Li, M.; Tang, B.; Tang, X. F.,

Proteomic analysis of the secretome of haloarchaeon Natrinema sp. J7-2. *Journal of proteome*

research **2014,** *13* (3), 1248-58.

55.   Hand, N. J.; Klein, R.; Laskewitz, A.; Pohlschroder, M., Archaeal and bacterial SecD and SecF

homologs exhibit striking structural and functional conservation. *Journal of bacteriology* **2006,** *188*

(4), 1251-9.

56.   Fink-Lavi, E.; Eichler, J., Identification of residues essential for the catalytic activity of

Sec11b, one of the two type I signal peptidases of Haloferax volcanii. *FEMS microbiology letters*

2008, *278* (2), 257-60.

57.   Gupta, R.; Brunak, S., Prediction of glycosylation across the human proteome and the

correlation to protein function. *Pacific Symposium on Biocomputing. Pacific Symposium on*

Biocomputing **2002**, 310-22.

58. Urban, S.; Dickey, S. W., The rhomboid protease family: a decade of progress on function and mechanism. *Genome biology* **2011,** *12* (10), 231.

59. Srivastava, P.; Kowshik, M., Mechanisms of metal resistance and homeostasis in haloarchaea. *Archaea* **2013,** 732864.

60. Reece, R. J.; Maxwell, A., DNA gyrase: structure and function. *Critical reviews in biochemistry and molecular biology* **1991,** *26* (3-4), 335-75.

61. Bush, N. G.; Evans-Roberts, K.; Maxwell, A., DNA Topoisomerases. *EcoSal Plus* 2015; doi:10.1128/ecosalplus.ESP-0010-2014.

62. Heide, L., New aminocoumarin antibiotics as gyrase inhibitors. *International journal of medical microbiology : IJMM* **2014,** *304* (1), 31-6.

63. Kuraoka, I., Diversity of Endonuclease V: From DNA Repair to RNA Editing. *Biomolecules* **2015,** *5* (4), 2194-206.

64. Woods, W. G.; Dyall-Smith, M. L., Construction and analysis of a recombination-deficient (radA) mutant of Haloferax volcanii. *Molecular microbiology* **1997,** *23* (4), 791-7.

65. Cheng, T. L.; Wu, Y. T.; Lin, H. Y.; Hsu, F. C.; Liu, S. K.; Chang, B. I.; Chen, W. S.; Lai, C. H.; Shi, G. Y.; Wu, H. L., Functions of rhomboid family protease RHBDL2 and thrombomodulin in wound healing. *The Journal of investigative dermatology* **2011,** *131* (12), 2486-94.

66. Kandiba, L.; Lin, C. W.; Aebi, M.; Eichler, J.; Guerardel, Y., Structural characterization of the N-linked pentasaccharide decorating glycoproteins of the halophilic archaeon Haloferax volcanii. *Glycobiology* **2016,** *26* (7), 745-56.

67.　　Tripepi, M.; You, J.; Temel, S.; Onder, O.; Brisson, D.; Pohlschroder, M., N-glycosylation of Haloferax volcanii flagellins requires known Agl proteins and is essential for biosynthesis of stable flagella. *Journal of bacteriology* **2012,** *194* (18), 4876-87.

68.　　Esquivel, R. N.; Schulze, S.; Xu, R.; Hippler, M.; Pohlschroder, M., Identification of Haloferax volcanii Pilin N-Glycans with Diverse Roles in Pilus Biosynthesis, Adhesion, and Microcolony Formation. *The Journal of biological chemistry* **2016,** *291* (20), 10602-14.

69.　　Kaminski, L.; Guan, Z.; Yurist-Doutsch, S.; Eichler, J., Two distinct N-glycosylation pathways process the Haloferax volcanii S-layer glycoprotein upon changes in environmental salinity. *mBio* **2013,** *4* (6), e00716-13.

70.　　Kandiba, L.; Guan, Z.; Eichler, J., Lipid modification gives rise to two distinct Haloferax volcanii S-layer glycoprotein populations. *Biochimica et biophysica acta* **2013,** *1828* (3), 938-43.

71.　　Abdul Halim, M. F.; Pfeiffer, F.; Zou, J.; Frisch, A.; Haft, D.; Wu, S.; Tolic, N.; Brewer, H.; Payne, S. H.; Pasa-Tolic, L.; Pohlschroder, M., Haloferax volcanii archaeosortase is required for motility, mating, and C-terminal processing of the S-layer glycoprotein. *Molecular microbiology* **2013,** *88* (6), 1164-75.

72.　　Esquivel, R. N.; Xu, R.; Pohlschroder, M., Novel archaeal adhesion pilins with a conserved N terminus. *Journal of bacteriology* **2013,** *195* (17), 3808-18.

73.　　Knopf, R. R.; Feder, A.; Mayer, K.; Lin, A.; Rozenberg, M.; Schaller, A.; Adam, Z., Rhomboid proteins in the chloroplast envelope affect the level of allene oxide synthase in Arabidopsis thaliana. *The Plant journal : for cell and molecular biology* **2012,** *72* (4), 559-71.

74.   Riestra, A. M.; Gandhi, S.; Sweredoski, M. J.; Moradian, A.; Hess, S.; Urban, S.; Johnson, P.

J., A Trichomonas vaginalis Rhomboid Protease and Its Substrate Modulate Parasite Attachment

and Cytolysis of Host Cells. *PLoS pathogens* **2015,** *11* (12), e1005294.

1
2
3
4
5
6
7
8
9
10
11
12
13
14
15
16
17
18
19
20
21
22
23
24
25
26
27
28
29
30
31
32
33
34
35
36
37
38
39
40
41
42
43
44
45
46
47

Table 1. Differential subproteome of the *H volcanii* MIG1 strain. Regulation factors for three biological replicates from H26 and MIG1 strains were submitted to a Student's t-test. Proteins with *p*-values ≤ 0.05 were considered significant. Negative fold values indicate that the protein is less abundant in the mutant than in the wt whereas a positive fold value indicates accumulation of the protein in MIG1. For membrane fractions two independent experiments (three biological replicates each) were performed and data corresponding to both assays was included in the table. TMS: number of transmembrane segments. Sec: general translocation signal peptide. Tat: Twin arginine translocation signal peptide. FC and SC: functional class and functional sub-class, according to the Halolex database, respectively (for abbreviations see Fig. 1).

ID	Gene name	Description	TMS	Signal peptide	Lipobox	FC	SC	*p* value	Fold
Supernatant Exponential									
HVO_0874	-	Beta-lactamase domain protein/mRNA 3-end processing factor homolog				MIS	GEN	0.000136	17.8
HVO_2375	*pstS1*	ABC-type transport system periplasmic substrate-binding protein (probable substrate phosphate)		Tat	Yes	TP_CP	TP	0.000013	11.4
HVO_2563	*rpl4*	50S ribosomal protein L4				GIP	TL	0.047086	1.7
Membrane Exponential									

HVO_1038	udg4	Uracil-DNA glycosylase superfamily protein			MIS	GEN	0.000666	28.7
HVO_1344	-	SBDS family protein			MIS	GEN	0.001658	18.1
HVO_2150	hcpG	Halocyanin	1	Tat	MET	EM	0.000016	7.8
HVO_2464	sucD	Succinate--CoA ligase (ADP-forming) alpha subunit			MET	CIM	0.041494	7.1
HVO_1925	-	Probable GTP-binding protein			MIS	GEN	0.042352	2.6
HVO_2757	rpl1	50S ribosomal protein L1			GIP	TL	0.008677	1.9
HVO_0316	atpA	A-type ATP synthase subunit A			MET	EM	0.049824	1.6
HVO_0570	-	Histidine kinase	3	Sec	ENV	SIG	0.043555	-1.5
HVO_0684	gatB, aatB	Aspartyl/glutamyl-tRNA(Asn/Gln) amidotransferase subunit B			GIP	TL	0.020533	-1.5
HVO_A0045	htpX3	HtpX-like protease	4		MIS	MIS	0.024904	-1.6
HVO_A0208	cas5	CRISPR-associated endoribonuclease Cas5, Hmari subtype			MIS	MIS	0.005354	-1.6
HVO_0194	orc9	Orc1-type DNA replication protein			MIS	MIS	0.026537	-1.8
HVO_0237	-	UPF0761 family protein			MIS	GEN	0.029733	-1.8
HVO_1357	-	receiver/bat box HTH-10 family transcription regulator			ENV	REG	0.04533	-1.8
HVO_B0052	-	PQQ repeat protein			MIS	GEN	0.043425	-1.9
HVO_0581	ftsZ2	cell division protein FtsZ, type II			MIS	MIS	0.024353	-2
HVO_1554	traB	TraB family protein	8		MIS	GEN	0.026824	-2
HVO_0874	-	beta-lactamase domain protein/mRNA 3-end processing factor homolog			MIS	GEN	0.045002	-2.6

HVO_0598	-	conserved hypothetical protein			UNASS	CHY	0.000252	-7.1
HVO_0762	-	NUDIX family hydrolase			MIS	GEN	0.000355	-8.4
HVO_1659	mscS2	mechanosensitive channel protein MscS	5	Sec	TP_CP	TP	0.000240	-9
HVO_1997	-	Abi/CAAX family protein	7		MIS	GEN	0.026824	-10.7
HVO_0255	-	Spermine/spermidine synthase family protein	7		MIS	GEN	0.000011	-10.8
HVO_0477	pepB3	Aminopeptidase (homolog to leucyl aminopeptidase / aminopeptidase T)			MIS	GEN	0.000214	-13.1
HVO_B0273	-	Sensor box histidine kinase	7		ENV	SIG	0.047159	-13.9
HVO_1382	nac	Nascent polypeptide-associated complex protein			GIP	TL	0.003979	-14.9
HVO_2060	agl8	NUDIX family hydrolase (low-salt glycan biosynthesis protein Agl8)			MIS	MIS	0.034081	-19.3
HVO_0941	-	Conserved hypothetical protein	6		UNASS	CHY	0.000550	-24.1
HVO_2318	uppS2	Tritrans,polycis-undecaprenyl-diphosphate synthase			MET	LIP	0.043265	-25.4
HVO_1676	tfb2	Transcription initiation factor TFB			GIP	TC	0.006282	-27.1
HVO_0408	-	PrsW family protein	9		MIS	GEN	0.000165	-28.2
Cytoplasm Exponential								
HVO_2548	rpl6	50S ribosomal protein L6			GIP	TL	0.000076	9.5
HVO_2772	-	rhodanese domain protein / probable metallo-beta-lactamase family hydrolase			MIS	GEN	0.000001	9.2
HVO_C0074	dppDF16	ABC-type transport system ATP-binding protein (probable			TP_CP	TP	0.000001	9.2

		substrate dipeptide/oligopeptide)				
HVO_2600	*map*	methionyl aminopeptidase	MIS	MIS	0.000035	8.5
HVO_1758	*trxB5*	oxidoreductase (homolog to thioredoxin-disulfide reductase)	MIS	GEN	0.000004	7.8
HVO_2709	-	GNAT family acetyltransferase	MIS	GEN	0.000104	6.9
HVO_0818	*thrC2*	threonine synthase	MET	AA	0.049049	4.9
HVO_1047	*qor2*	NADPH:quinone reductase	MIS	MIS	0.047097	4.8
HVO_1604	*aspC1*	pyridoxal phosphate-dependent aminotransferase (probable aspartate aminotransferase)	MIS	GEN	0.044358	2
HVO_A0406	-	conserved hypothetical protein	UNASS	CHY	0.010564	2
HVO_2270	*rmeM*	type I restriction-modification system DNA-methyltransferase RmeM	MIS	MIS	0.008658	1.9
HVO_0353	*rps12*	30S ribosomal protein S12	GIP	TL	0.024019	1.8
HVO_1478	*tfb5*	transcription initiation factor TFB	GIP	TC	0.049709	1.7
HVO_1681	-	DNA N-glycosylase	GIP	RRR	0.038567	1.6
HVO_2345	-	flavin-dependent pyridine nucleotide oxidoreductase	MIS	GEN	0.041979	1.6
HVO_0710	*pabB*	aminodeoxychorismate synthase component II	MET	COM	0.049446	1.5
HVO_1249	-	conserved hypothetical protein	MIS	GEN	0.025429	1.5
HVO_1488	*gnaD*	D-gluconate dehydratase	MET	CHM	0.002489	-1.5
HVO_A0379	*hyuA2*	N-methylhydantoinase A(ATP-hydrolyzing)	MIS	MIS	0.013225	-1.5
HVO_2790	*apbC1*	Fe-S cluster carrier protein ApbC	MIS	MIS	0.012758	-1.6

HVO_2059	*agl12,* *rfbB*	dTDP-glucose 4,6-dehydratase (Agl12)				MET	CHM	0.036699	-1.7
HVO_2947	*pheT*	phenylalanine--tRNA ligase beta subunit				GIP	TL	0.0382	-1.8
HVO_0214	-	L-lactate dehydrogenase		Sec		MET	CIM	0.004094	-1.9
HVO_2695	*tsgA3*	ABC-type transport system periplasmic substrate-binding protein (probable substrate sugar)		Tat	Yes	TP_CP	TP	0.027275	-2
HVO_1401	*tsgA11*	ABC-type transport system periplasmic substrate-binding protein (probable substrate sugar)		Tat	Yes	TP_CP	TP	0.003844	-2.1
HVO_2740	*ndk*	nucleoside-diphosphate kinase				MET	NUM	0.019173	-2.2
HVO_1311	-	probable oxidoreductase (short-chain dehydrogenase family)				MIS	GEN	0.032821	-6
HVO_2684	-	UspA domain protein				MIS	GEN	0.000151	-9.1
HVO_2648	*serA2*	phosphoglycerate dehydrogenase				MIS	GEN	0.000035	-9.4
Supernatant Stationary									
HVO_0062	*dppA1*	ABC-type transport system periplasmic substrate-binding protein (probable substrate dipeptide/oligopeptide)		Tat	Yes	TP_CP	TP	0.031260	1.7
HVO_1976	*secD*	Protein-export membrane protein SecD	5	Sec		TP_CP	SEC	0.047004	-5.3
HVO_1210	*flgA1*	Flagellin 1	1			TP_CP	MOT	0.000004	-5.3
HVO_1477	-	Endonuclease domain protein		Sec	Yes	MIS	GEN	0.000004	-5.3
HVO_2607	-	PQQ repeat protein		Tat	Yes	MIS	GEN	0.000004	-5.3
HVO_0058	*dppF1*	ABC-type transport system ATP-binding protein (probable				TP_CP	TP	0.000086	-6.0

		substrate dipeptide/oligopeptide)							
HVO_A0181	-	Conserved hypothetical protein		Tat	Yes	UNASS	CHY	0.000369	-6.0
HVO_A0377	*hyuE*	Hydantoin racemase				MIS	MIS	0.000608	-6.5
HVO_2384	-	CBS domain protein				MIS	GEN	0.000010	-6.7
HVO_2603	*sec11a*	Signal peptidase I	1			TP_CP	SEC	0.000010	-6.7
HVO_1945	-	Conserved hypothetical protein		Tat	Yes	UNASS	CHY	0.000144	-6.7
HVO_2413	*tef1a2*	Translation elongation factor aEF-1 alpha subunit				GIP	TL	0.035008	-7.0
HVO_2286	-	Conserved hypothetical protein		Tat	Yes	UNASS	CHY	0.027060	-7.4
HVO_1153	-	Conserved hypothetical protein	1			UNASS	CHY	0.000002	-7.5
HVO_0054	*glyS*	Glycine--tRNA ligase				GIP	TL	0.000377	-7.8
HVO_B0057	*cbiH2, cobJ2*	Precorrin-3B C17-methyltransferase				MET	COM	0.000124	-8.7
HVO_2815	*hbd1*	3-hydroxyacyl-CoA dehydrogenase / enoyl-CoA hydratase				MET	LIP	0.000706	-8.9
HVO_0348	*rpoB1*	DNA-directed RNA polymerase subunit B'				GIP	TC	0.000865	-9.0
HVO_2471	*pccB2*	Propionyl-CoA carboxylase carboxyltransferase component				MET	LIP	0.033685	-9.1
HVO_2554	*rpl14*	50S ribosomal protein L14				GIP	TL	0.000011	-9.5
HVO_B0184	*dppA14*	ABC-type transport system periplasmic substrate-binding protein (probable substrate dipeptide/oligopeptide)		Tat	Yes	TP_CP	TP	0.000573	-10.1
HVO_B0061	*cbiL*	Precorrin-2 C20-methyltransferase				MET	COM	0.000175	-10.2
HVO_2749	*rpl21e*	50S ribosomal protein L21e				GIP	TL	0.000001	-10.3

HVO_2452	*nrdJ*	Ribonucleoside-diphosphate reductase, adenosylcobalamin-dependent			MET	NUM	0.036975	-11.9
Membrane Stationary								
HVO_0887	*korB*	oxoglutarate--ferredoxin oxidoreductase beta subunit			MET	CIM	0.006496	1.7
HVO_2614	*udp2*	uridine phosphorylase			MET	NUM	0.023086	1.5
HVO_2989	*pmm4*	phosphohexomutase (phosphoglucomutase / phosphomannomutase)			MET	CHM	0.040726	-1.5
HVO_2069	-	RND superfamily permease	11		TP_CP	TP	0.002656	-1.6
HVO_C0054	-	hypothetical protein		Tat	UNASS	HY	0.033063	-1.6
HVO_0307	-	conserved hypothetical protein		Sec	UNASS	CHY	0.022016	-2
HVO_1751	*copA*	P-type transport ATPase (probable substrate copper/metal cation)	8		TP_CP	TP	0.011109	-2.1
HVO_0462	*cydA*	cytochrome bd ubiquinol oxidase subunit I	9		MET	EM	0.000721	-8.8
HVO_B0228	*tsgA9*	ABC-type transport system periplasmic substrate-binding protein (probable substrate sugar)		Tat	Yes	TP_CP	TP	0.000374	-8.8
HVO_1870	-	probable metalloprotease	7		MIS	GEN	0.000041	-9.9
Cytoplasm Stationary								
HVO_1804	*pncB*	nicotinate phosphoribosyltransferase			MET	COM	0.000018	8.2
HVO_2639	-	DUF1611 family protein			MIS	GEN	0.0001	6.7
HVO_2860	-	DUF181 family protein			MIS	GEN	0.0001	6.7

1
2
3
4
5
6
7
8
9
10
11
12
13
14
15
16
17
18
19
20
21
22
23
24
25
26
27
28
29
30
31
32
33
34
35
36
37
38
39
40
41
42
43
44
45
46
47

HVO_0087	*hemB*	porphobilinogen synthase	MET	COM	0.0376	-1.5
HVO_1575	*rocF*	Arginase	MET	AA	0.0356	-1.5
HVO_2225	-	AstE family protein	MIS	GEN	0.0232	-1.8

1
2
3
4
5
6
7
8
9
10
11
12
13
14
15
16
17
18
19
20
21
22
23
24
25
26
27
28
29
30
31
32
33
34
35
36
37
38
39
40
41
42
43
44
45
46
47

Table 2. Proteins with differential migration in SDS-PAGE in the MIG1 mutant. Membrane protein samples (triplicates) from exponentially growing MIG1 and wt cells were subjected to SDS-PAGE allowed to run for 2 cm and separated in four sections (top to bottom: S1-S4) which were analyzed separately by RPLC-MS/MS, as indicated in Table 1. Regulation factors were submitted to a Student's t-test and proteins with p-values ≤ 0.05 and fold ≥ 1.5 were considered significant. In grey, integral membrane proteins. Ns: not significant.

ID	Gene name	Protein name	TMS	Signal peptide	Lipobox	FC	SC	Fold S1	Fold S2	Fold S3	Fold S4	Total Fold
HVO_1240	-	Conserved hypothetical protein	0	Tat	Yes	UNASS	CHY	8.8		1.8		ns
HVO_2545	rpl18	50S ribosomal protein L18	0			GIP	TL	8.1				ns
HVO_2302	-	Ubiquinone biosynthesis protein UbiB	3			MET	COM	1.8				ns
HVO_1847	pepF	Oligoendopeptidase PepF	0			MIS	MIS	1.7				ns
HVO_2495	-	DUF106 family protein	4			MIS	GEN	-1.5				ns
HVO_0541	citB2. acnA	aconitate hydratase	0			MET	CIM	-1.5				ns
HVO_C0075	dppA16	ABC-type transport system periplasmic substrate-binding protein (probable substrate dipeptide/oligopeptide)	0	Tat	Yes	TP_CP	TP	-1.5				ns
HVO_1469	menD	2-succinyl-5-enolpyruvyl-6-hydroxy-3-cyclohexene-1-carboxylate synthase	0			MET	COM	-1.6				-1.9
HVO_1242	-	Conserved hypothetical protein	0	Tat	Yes	UNASS	CHY	-7.8				ns
HVO_0893	mmcA1	Methylmalonyl-CoA mutase subunit A	0			MET	CIM	-10.3				ns
HVO_C0074	dppDF16	ABC-type transport system ATP-binding protein (probable substrate dipeptide/oligopeptide)	0			TP_CP	TP	-14.4				ns
HVO_0519	rpa2	Replication protein A	0			GIP	RRR			7.1		ns

HVO_2784	rps13	30S ribosomal protein S13	0			GIP	TL	5.2		ns
HVO_0447	phnD1	ABC-type transport system periplasmic substrate-binding protein (probable substrate phosphate/phosphonate)	0	Tat	Yes	TP_CP	TP	2.1		2.0
HVO_2945	valS	Valine--tRNA ligase	0			GIP	TL	1.8		ns
HVO_0220	mcm	ATP-dependent DNA helicase MCM	0			GIP	RRR	1.8		ns
HVO_1305	porA	Pyruvate--ferredoxin oxidoreductase alpha subunit	0			MET	CIM	1.8		ns
HVO_0133	ths1. cct1	Thermosome subunit 1	0			GIP	CHP	1.7		ns
HVO_1590	dnaK	DnaK-type molecular chaperone Hsp70	0			GIP	CHP	1.6		ns
HVO_2072	csg	S-layer glycoprotein	1	Sec		TP_CP	CE	1.5	1.7	ns
HVO_0717	ftsZ1	Cell division protein FtsZ. type I	0			TP_CP	CP	1.5		ns
HVO_2209	oadhA4	Probable branched-chain amino acid dehydrogenase E1 component alpha subunit	0			MET	AA	-1.5		-1.6
HVO_A0379	hyuA2	N-methylhydantoinase A(ATP-hydrolyzing)	0			MIS	MIS	-1.5		ns
HVO_1304	porB	Pyruvate--ferredoxin oxidoreductase beta subunit	0			MET	CIM	-1.5		ns
HVO_0481	gap2	Glyceraldehyde-3-phosphate dehydrogenase (NAD) (phosphorylating)	0			MET	CIM	-1.5		ns
HVO_A0271	glpC2	Glycerol-3-phosphate dehydrogenase subunit C	0			MET	CIM	-1.5		-1.7
HVO_3007	mdh	Malate dehydrogenase	0			MET	CIM	-1.6		ns
HVO_1009	-	Probable oxidoreductase (aldo-keto reductase family protein)	0			MIS	GEN	-1.6	1.6	ns
HVO_2617	-	TrkA-C domain protein	3			MIS	GEN	-1.7		ns
HVO_2643	qor1	NADPH:quinone reductase	0			MIS	MIS	-1.7		ns
HVO_0243	ltaE	Threonine aldolase	0			MET	AA	-1.8		-1.9

HVO_0832	-	Alpha/beta hydrolase fold protein	0	Sec		MIS	GEN	-1.8	-1.8	-1.6
HVO_0945	cbaA	ba3-type terminal oxidase subunit I	14			MET	EM	-1.8		ns
HVO_0104	radA	DNA repair and recombination protein RadA	0			GIP	RRR	-1.9		ns
HVO_1573	gyrA	DNA gyrase subunit A	0			GIP	RRR	-2.2		ns
HVO_1631	dph2	S-adenosyl-L-methionine:L-histidine 3-amino-3-carboxypropyltransferase (GTP binding)	0			MIS	MIS	-5.2	5.8	ns
HVO_1675	corA	Magnesium transport protein CorA	2			TP_CP	TP	-5.2		-1.7
HVO_B0078	dppF11	ABC-type transport system ATP-binding protein (probable substrate dipeptide/oligopeptide)	0			TP_CP	TP	-5.4	13.6	ns
HVO_1443	-	ABC-type transport system ATP-binding protein	0			TP_CP	TP	-5.5		-2.0
HVO_2191	purU	Formyltetrahydrofolate deformylase	0			MET	NUM	-5.8		ns
HVO_1006	-	ABC-type transport system ATP-binding protein	0			TP_CP	TP	-6.3		ns
HVO_B0011	soxA1	Sarcosine oxidase	0			MET	AA	-6.3		-6.7
HVO_2168	moxR3	AAA-type ATPase (MoxR subfamily)	0			MIS	MIS	-6.4	13.8	ns
HVO_0951	-	Hypothetical protein	1			UNASS	HY	-6.5		-6.9
HVO_2993	pibD	Prepilin peptidase PibD	6			MIS	MIS	-7.7		-2.0
HVO_2348	mptA. folE2	GTP cyclohydrolase MptA	0			MET	COM	-12.4	9.0	-1.7
HVO_1576	-	NAD-dependent epimerase/dehydratase	0			MIS	GEN		17.4	2.3
HVO_2397	znuA1	ABC-type transport system periplasmic substrate-binding protein (probable substrate zinc)	0	Tat	Yes	TP_CP	TP		14.6	ns
HVO_A0611	znuA2	ABC-type transport system periplasmic substrate-binding protein (probable substrate zinc)	0	Tat	Yes	TP_CP	TP		9.6	ns
HVO_2374	phoU2	Transcription regulator (homolog to phosphate uptake	0			ENV	REG		9.0	ns

		regulator)							
HVO_0739	-	Conserved hypothetical protein	4			UNASS	CHY	9.0	ns
HVO_2943	pyrD	Dihydroorotate dehydrogenase (quinone)	0			MET	NUM	7.9	ns
HVO_2607	-	PQQ repeat protein	0	Tat	Yes	MIS	GEN	7.3	ns
HVO_2384	-	CBS domain protein	0			MIS	GEN	7.1	ns
HVO_2068	ftsZ8	FtsZ family protein. type III	0			MIS	GEN	6.1	ns
HVO_A0619	-	Conserved hypothetical protein	0	Tat	Yes	UNASS	CHY	5.8	ns
HVO_2756	rpl10	50S ribosomal protein L10	0			GIP	TL	5.1	ns
HVO_1506	ilvC	Ketol-acid reductoisomerase	0			MET	AA	2.7	ns
HVO_1570	top6A	DNA topoisomerase VI subunit	0			GIP	RRR	2.4	ns
HVO_0059	dppD1	ABC-type transport system ATP-binding protein (probable substrate dipeptide/oligopeptide)	0			TP_CP	TP	1.9	ns
HVO_2046	agl7	Sulfatase domain protein	0			MIS	MIS	1.8	ns
HVO_2047	-	Conserved hypothetical protein	0			UNASS	CHY	-1.5	ns
HVO_2703	panB2	3-methyl-2-oxobutanoate hydroxymethyltransferase	0			MET	COM	-1.6	-1.5
HVO_2544	rps5	30S ribosomal protein S5	0			GIP	TL	-1.6	ns
HVO_0790	fba2	2-amino-3.7-dideoxy-D-threo-hept-6-ulosonate synthase	0			MET	AA	-1.6	ns
HVO_1751	copA	P-type transport ATPase (probable substrate copper/metal cation)	8			TP_CP	TP	-1.7	-1.7
HVO_0841	petD	Cytochrome bc1 complex cytochrome b/c subunit	5			MET	EM	-1.7	ns
HVO_0773	-	Probable S-adenosylmethionine-dependent methyltransferase	0			MIS	GEN	-1.7	ns
HVO_2398	znuC1	ABC-type transport system ATP-binding protein (probable	0			TP_CP	TP	-1.7	-1.6

		substrate zinc)							
HVO_1478	*tfb5*	Transcription initiation factor TFB	0			GIP	TC	-1.8	ns
HVO_B0134	-	ABC-type transport system ATP-binding protein	0			TP_CP	TP	-1.8	-1.7
HVO_2554	*rpl14*	50S ribosomal protein L14	0			GIP	TL	-1.8	ns
HVO_2981	*upp*	Uracil phosphoribosyltransferase	0			MET	NUM	-1.9	ns
HVO_1241	*prrC*	SCO1/SenC/PrrC family protein	0	Tat	Yes	MIS	GEN	-2.0	-1.5
HVO_0536	*dpsA1*	Ferritin	0			MIS	MIS	-2.2	ns
HVO_0727	-	Rhomboid protease II	6			MIS	GEN	-6.6	-6.7
HVO_1274	-	Conserved hypothetical protein	7			UNASS	CHY	-6.6	-5.5
HVO_1532	-	DUF368 family protein	8			MIS	GEN	-6.6	ns
HVO_1914	*acaB3*	Acetyl-CoA C-acyltransferase	0			MET	LIP	-7.4	-5.1
HVO_1936	*cofE*	F420-0:gamma-glutamyl ligase	0			MET	COM	-7.4	-6.1
HVO_2318	*uppS2*	Tritrans.polycis-undecaprenyl-diphosphate synthase	0			MET	LIP	-7.5	ns
HVO_2055	*agl15*	Probable low-salt glycan biosynthesis flippase Agl15	14			TP_CP	TP	-8.1	ns
HVO_2602	-	Transport protein (probable substrate zinc/cadmium)	4			TP_CP	TP	-8.4	-6.9
HVO_2952	*endA*	tRNA-splicing endonuclease	0			GIP	RMT	-8.4	-6.9
HVO_0972	*pilA1*	Pilin (PilA1)	1			MIS	MIS	11.7	2.0
HVO_2773	*rps2*	30S ribosomal protein S2 1	0			GIP	TL	10.6	ns
HVO_0531	*tsgB1*	ABC-type transport system permease protein (probable substrate sugar)	0			TP_CP	TP	8.6	ns
HVO_1110	*btuF*	ABC-type transport system periplasmic substrate-binding protein (probable substrate cobalamin)	0	Sec		TP_CP	TP	7.1	ns
HVO_2163	-	ABC-type transport system ATP-binding protein (homolog	0			TP_CP	TP	7.1	ns

		to LolDCE lipoprotein release factor)						
HVO_2547	*rpl32e*	50S ribosomal protein L32e	0		GIP	TL	1.9	ns
HVO_2564	*rpl3*	50S ribosomal protein L3	0		GIP	TL	1.7	ns
HVO_0316	*atpA*	A-type ATP synthase subunit A	0		MET	EM	1.6	ns
HVO_0060	*dppC1*	ABC-type transport system permease protein (probable substrate dipeptide/oligopeptide)	8		TP_CP	TP	-1.5	ns
HVO_B0185	*dppB14*	ABC-type transport system permease protein (probable substrate dipeptide/oligopeptide)	6		TP_CP	TP	-1.6	ns
HVO_0500	-	Conserved hypothetical protein	1		UNASS	CHY	-1.6	ns
HVO_1198	-	UspA domain protein	0		MIS	GEN	-1.8	ns
HVO_0146	*psd*	Phosphatidylserine decarboxylase	1		MET	LIP	-2.5	ns
HVO_1563	-	Conserved hypothetical protein	0	Sec	UNASS	CHY	-2.6	-1.6
HVO_1377	-	UPF0145 family protein	0		MIS	GEN	-13.4	-6.9

1
2
3
4
5
6
7
8
9
10
11
12
13
14
15
16
17
18
19
20
21
22
23
24
25
26
27
28
29
30
31
32
33
34
35
36
37
38
39
40
41
42
43
44
45
46
47

For table of contents only